Effect of Delta–Winglet Vortex Generators on a Forced Convection Heat Transfer in an Asymmetrically Heated Triangular Duct

Mohanad A. Al-Taher , Adnan A. Abdul-Rassol and Hamid E.Zangana
Dept.of Mech.Eng.College of Engineer.University of Al- Anbar.

ABSTRACT

An experimental investigation is performed to study the friction factor (f) and convection heat transfer coefficient (h) behavior in an asymmetrically heated equilateral triangular duct by using delta–winglets vortex generators which are embedded in a turbulent boundary layer. Two side walls of the heated test section are electrically heated with a constant heat flux, whereas the lower wall is indirectly heated. Reynolds number (Re) is ranged from (23,000) to (58,000). Two sizes and three attack angles of vortex generators are studied here for three cases; single, double, and treble pairs of generators. Each pair was supported in one wall of the test section at the various locations from the leading edge. The indicated results that friction factor (f)and Nusselt number (Nu) are relatively proportion with the size, number and the inclination angle of the generators. The (f) decreases as airflow rate increases whereas Nu number increases. The present data of (f) is less than the data of Chegini by about (6.5 %) and overpredicts the data of Altemani by about (1.7 %).

Keyword: Heat Transfer Enhancement, Noncircular ducts, Delta-Winglet Vortex Generators, Turbulent Flow.

تاثير توليد الدوران على انتقال الحرارة القسري في مجرى مثلث مسخن تسخينا غير متجانس

مهند عبد الفتاح الظاهر و عدنان عبد الامير عبد الرسول و حمدي عماد الدين احمد
قسم الهندسة الميكانيكية – كلية الهندسة– جامعة الانبار

الخلاصة:

يتناول هذا البحث دراسة تجريبية لسلوك معامل الاحتكاك و تحسين معامل انتقال الحرارة بالحمل ألقسري (ممثلاً بعدد نسلت Nu) في مجرى مثلث المقطع مسخن تسخيناً غير متجانس باستخدام مولدات الدوامية نوع (Delta-Winglet) مغمورة في الطبقة المتآخمة المضطربة. إن الجدارين الجانبيين لمقطع الاختبار مسخنان تسخيناً كهربائياً معتمِدِينَ ثبوت الفيض الحراري كشرطٍ حدي، في حين أن الجدار السفلي مسخن بطريقة غير مباشرة. تراوح عدد رينولدز بين (٢٣.٠٠٠) إلى (٥٨.٠٠٠) خلال التجارب المختبرية. تم دراسة حجمين وثلاث زوايا لمولد الدوامية ولثلاث حالات والتي هي؛ زوج مفرد وزوجين وثلاثة أزواج من مولدات الدوامية حيث تم تثبيت كل زوج على السطح الداخلي لجدار مقطع الاختبار عند مسافات مختلفة من حافة المقدمة. لوحظ أن معامل الاحتكاك (f) ورقم نسلت (Nu) تناسبا طرديا مع حجم مولدات الدوامية وعددها وزاوية انحرافها، بينما يتناقص معامل الاحتكاك مع زيادة معدل تدفق الهواء في حين أن عدد نسلت يتزايد طرديا. تم استخراج معادلات إرتباطية لمعظم الحالات ولكل من معامل الاحتكاك وعدد نسلت وقد وجد أن معامل الاحتكاك كان اقل من القيم التي أوجدها الباحث Chegini بحوالي (٦.٥%) وأعلى من تلك التي أوجدها الباحث Altemani بحوالي (١.٧%).

1. INTRODUCTION

The fluid flow and heat transfer characteristics of non–circular duct have been studied extensively in the past five decades to wide applications in the compact heat exchangers, solar collector, laser curtain seals, and cooling of electrical devices. But in these applications, gases are used instead of liquids as heat transfer medium. Gases inherently have lower heat transfer rates than liquids; therefore, heat transfer enhancement techniques that maximize heat transfer are of particular interest. The former investigators studied the techniques of heat transfer augmentation theoretically and experimentally and they found that the only effective method which increases the heat transfer coefficient is to decrease the thermal resistance of the sublayer adjacent to the wall immediately (i.e., the viscous effects of the sublayer are dominant). This can be achieved by increasing the turbulence in the main stream so that the turbulent eddies can penetrate deeper into this layer [**1,2].**

Many investigators investigated the pressure drop and heat transfer characteristics in a duct with a non–circular cross–section and they found that the pressure drop in a fully developed turbulent flow can also be estimated in first approximation from a turbulent flow correlation of circular duct if the diameter is replaced by the hydraulic diameter of the particular cross–section. This is particularly true for turbulent flow in triangular ducts for which only minor deviation from circular tube correlations for friction factor Chegini and Chaturvedi (1986) [**3**]. Carlson and Irvine noted that the friction factor correlation for circular tube with a hydraulic diameter predicts values some (21) percent high for (4 deg) apex angle, and (5) percent high at a (38 deg) angle Rohsenow (1985) [**4**].

Fins are commonly used between the plates in such heat exchanger to increase their compactness and this often results in plate–fin flow passages of triangular cross–section, with small hydraulic diameter as seen in Figure (1).

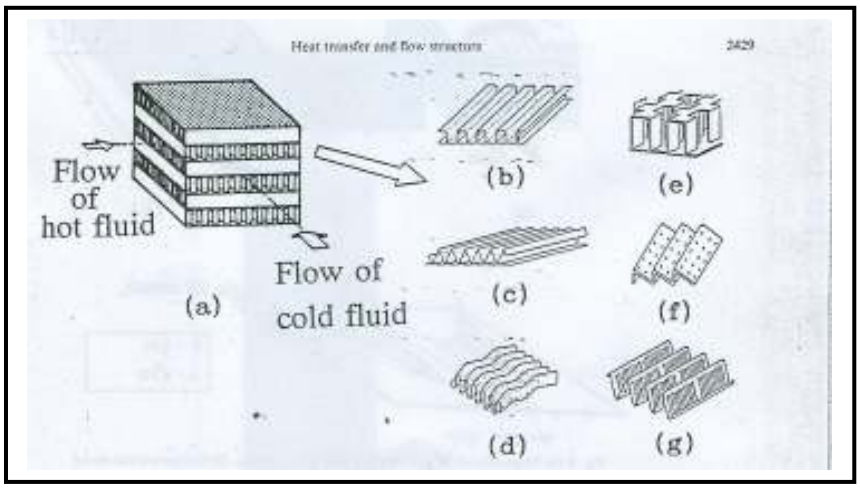

Fig. 1. (a) plate-fin heat exchanger and its surface geometries; (b) plain rectangular fins; (c) plain triangular fins; (d) wavy fins; (e) offset strip fins; (f) perforated fins and (g) louvered fins.

The other applications of the triangular ducts are the flat–plate solar collectors. As airflow heat transfer coefficients are much lower than those of water flow in the same boundary conditions, the circular tubes that are common in water–operated collectors have to be replaced with a duct configuration which affords greater heat transfer surface area. One such configuration is formed when the collector plate is a corrugated surface consisting of a succession of V–grooves. When the corrugated plate rests on the underside

insulation of the solar collector, an array of triangular ducts is created which constitute the passages of the airflow. The Nu number prediction for the isosceles triangular duct is shown a highest values for an apex–angle of (60 deg) Altemani and Sparrow (1980) [**5**]. According to this condition, a (60 deg) apex–angle is adopted in the experimental work.

The amount of heat transfer through a channel by convection is essentially depending on the thermal conductivity of the conductor surface, convection heat transfer coefficient of flowing fluid, the internal surface area that is exposed to convection heat transfer, and the fluid velocity. The increment in fluid motion enhances a heat transfer since it brings hotter and cooler layers of fluid into contact.

For reduction of thermal resistance, the heat transfer coefficient needs to be augmented by a way such using the vortex generators, which can be punched or attached with internal surface of the channel wall. The vortex generator generates longitudinal vortices along their leading edge. These vortices turn the flow field perpendicular to the main flow direction and enhance the fluid mixing and also to penetrate the fluid more through in the corners. These vortices also disrupt the growth of the thermal boundary layer and serve ultimately to bring about the enhancement of heat transfer between the fluid and the duct wall. However, there are generally four types of generators which are; rectangular wing, triangular wing, rectangular winglet pair, and delta winglet pair as shown in Figure (2).

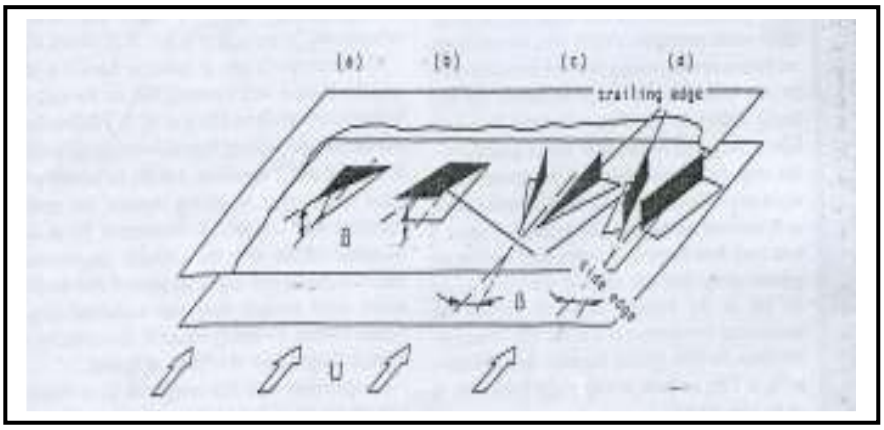

Fig. 2. Longitudinal vortex generators types; a- delta wing, b- rectangular wing, c- delta winglet pair, d–rectangular winglet pair [6].

The delta–winglet vortex generators are preferred for heat transfer augmentation applications in ducts as detected in an experimental comparison work, Pauley and Eaton (1994) [**6**], and Tiggelbeck, Mitra and Feibig (1994) [**7**]. The advantages of vortex generators is better compared with the fins (serves as extended surfaces). These advantages are of facility of fabrication, low cost, small size, and cause lower energy losses [**3**]. Many variables are studied here number of vortex, size, location, and angle of attack of generator.

2. EXPERIMENTAL APPARATUS

The apparatus works in an open–loop airflow circuit which takes air from building, and discharges it to the atmosphere, and it consists essentially of the blower, circular tube, contraction section, development section, test section, thermal mixing box, and heating

element. The air is drawn by the blower through a control valve which is used to adjust the amount of flow rate. The air is forced to flow through a circular galvanized iron tube which is provided by an orifice plate flowmeter to measure the flow rate. The upstream end of the circular tube is coupled with the blower by using a rubber tube to minimize the vibration that occurs during blower operation. Then the air passes through a hydrodynamic development section that has an equilateral triangular cross–section. The circular cross–section of the tube is converted to the triangular cross–section by using a convergent contraction section that is made from an aluminum sheet. The air passes through the test section and then through a thermal mixing chamber that is coupled with the end of the test section by a discharge section that it is long enough to ensure that the air is mixed well before entering to the mixing chamber and finally the air is exhausted outside of the building. The test section has a cross–section similar to that of development and discharge section and they are mated together.

2.1. Development Section

To reduce the turbulence of airflow when the air exits in a form of turbulence flow from the blower and then from the orifice plate, a long development section was employed. It has an equilateral triangular cross–section. The walls are constructed from a Plexiglass (the commercial name is known as Perspex), which is particularly selected to its transparency, light weight, surface smoothness, and availability in many sizes. The three walls are machined and connected by using a chemical binder. The three corners were externally sealed by using silicon sealant material to ensure the air tightness and prevent the leakage. The wall thickness, outer side length, hydraulic diameter, and the axial length of the development section are (7.0 mm), (80.0 mm), (35.7 mm), (1.20×10^3 mm, i.e., 33.6 D_h) respectively.

2.2. Heated Test Section

The test and development sections are horizontal, collinear, and shared a common internal hydraulic diameter throughout the experiments. The two–heated walls are of aluminum to obtain a uniform wall temperature at the circumferential of any cross–section of the heated wall. The unheated directly wall (lower wall) is of Perspex. The axial length of the test section equals to (1.50×10^3 mm) (i.e., 42.0 D_h), and the length of the contact region in cross–section between the heated and unheated wall is of (9.23 mm).

Nine grooves were machined by using milling machine on the outer surface of the heated walls at their axial length with cross–section of (2.0 mm) depth, and (3.0 mm) width to place the heater element through in. Each heated wall is heavily drilled in more than (18) situations to install the thermocouples through in with hole diameter of (1.50 mm) and depth of (5.0 mm) as illustrated in Figure (3). The outer surface of the heated walls was sprayed with layer of electrical insulation to insure no contact between the heater and groove. All test section walls are connected together by using six binders of aluminum which are uniformly distributed at the axial length of the test section. The corners of the test section are coated at the outer surface with silicon sealant to prevent the air leakage and ensure the tightness. Also, the inner surface of the heated walls was hand polished to a high degree of smoothness.

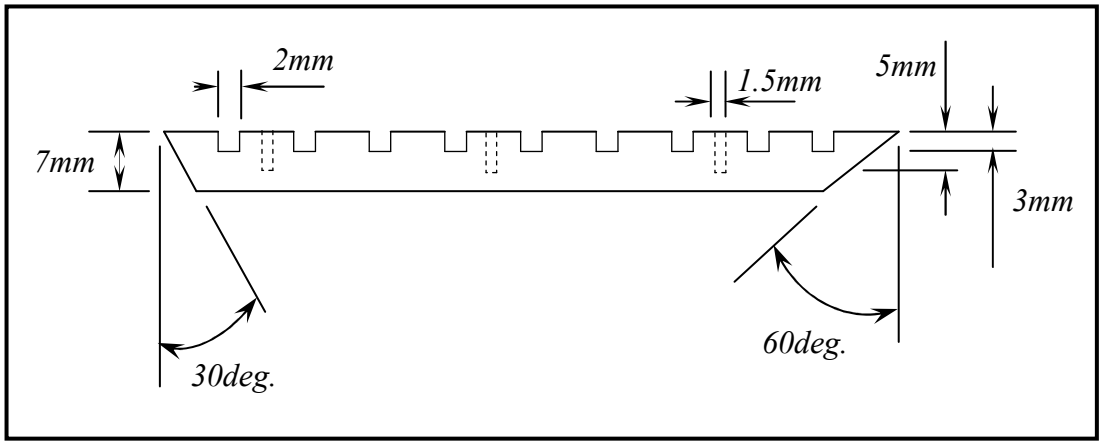

Fig. 3. The machining operations of the heated wall.

2.3. External Thermal Insulation of the Heated Test Section

The test section is heavily insulated to minimize the heat losses (i.e., to keep the heat transfer balance). It is enveloped with two successive layers of the glass wool (which has 0.038 W/m.^{o}C thermal conductivity) with layer thickness of (20 mm) and then placed through in a wooden box (the thermal conductivity of wood lath is 0.28 W/m. ^{o}C, [**8**]) with cross–section of (170 mm × 180 mm) to increase the outer thermal resistance. A cavity is created in the input and output of the wooden box with equilateral triangular cross section, while the test section is positioned centrally in the cavity cross section and then these two cavities were filled with glass wool to increase the insulation.

2.4. Thermal Mixing Chamber and Discharge Duct

Thermal mixing chamber is fabricated from the cork (k= 0.045 W/m. ^{o}C) **[8]** with thickness of (26.0 mm) to its high thermal resistance and connected with the test section by using a discharge duct with length of (600 mm, or 16.8 D_h), has the similar cross–section of the test and development sections. The metal of this duct is of Perspex, and the role of this section is to measure the pressure drop through the test section and to couple the mixing chamber with the test section immediately to ensure a good mixing of the outlet air from the heated duct. Therefore, the discharge duct is wrapped with one layer of the glass wool to ensure there is no heat losses and to keep the outlet air bulk temperature to be constant during air flow through this duct. One thermocouple is employed to sense the outlet bulk temperature which was mixed through in the mixing chamber and traversed immediately downstream end of mixing chamber to ensure that the air is mixing well.

2.5. Vortex Generator:

The aim of the present work is to enhance the heat transfer rate by using the vortex generators instead of fins, to its low manufacturing cost, small size, superiority in efficiency if a comparison is made with fins and also the need for such investigations because studies in this field of augmentation are rare. Longitudinal vortices are generated along their side edges by separation of the flow due to the pressure difference between the upstream and downstream side of the vortex generator. These vortices rotate the flow around the main flow direction and enhance mixing of the fluids close to and far from the wall. The vortices generation by using fins (as extended surfaces) is limited from the

economical consideration. If the fins are selected in the form of longitudinal vortex generators, then the additional heat transfer benefit coming from churning of the flow may exceed the benefit of increasing the heat transfer surface by fins.

The type of rectangular and delta winglet pair of vortex generator give higher augmentation in heat transfer coefficient and lower pressure drop than those of wing type, whereas the delta winglet pair causes lower pressure drop and gives higher heat transfer rate than that of rectangular winglet pair [**7**]. Therefore, the delta winglet pairs were selected to these advantages. One side of each winglet–pair is fixed on the bottom wall and the trailing edge of each is free. The angle of attack of the vortex generator can be varied to verify the effect of angle changing on the Nu number and (f) values. Two different geometries of vortex generators were used with dimension of (10 mm height, and 40 mm length) and (5.0 mm height, 27.5 mm length). The space between the pair of vortex generator is held to the (35 mm).

3. INSTRUMENTATION

3.1. Airflow Measurement

The airflow rate was measured by the orifice plate flowmeter, which is placed in the mid–length of the circular tube (at sufficient length to ensure that the fluctuating of the manometer reading for the pressure difference between the two sides of the orifice plate doesn't excess (0.4 mm) for the highest flow rates). The inner diameter ratio of the orifice plate to the tube diameter (D_o/D_t) is (0.7). The orifice plate flowmeter is designed according to the ISO 5167 orifice plate. To estimate the static pressure drop through the test section, three holes are drilled at ($4.2D_h$) upstream and another three at ($2.8D_h$) downstream end of the test section. Each side was provided with hole at mid–length and they are connected together with PVC tube which is connected with inclined manometer.

3.2. Temperature Measurement

The test section was provided by a system to measure the heated/unheated wall surface temperature (T_s), and the inlet/outlet air bulk temperature ($T_{b_{in}} / T_{b_{out}}$). The system essentially consisted of (40) thermo– couples (K) type (Chromel (positive)–Alomel (negative)), two for the inlet/outlet bulk temperatures and twenty eight for the heated wall temperatures. Ten thermocouples were installed in the bottom of the lower wall. Also to be more accurate, (16) thermocouples were distributed at the circumferential of the two heated walls uniformly at four situations to observe the distribution of circumferential temperatures. Thermocouples are adhered through in the holes by using steel epoxy, which is blended with steel powder to increase its conductivity. The junctions of the thermocouples are performed by melting the terminal of each thermocouple together by electrical spark which is consequent from the electrical discharge supply using a proper voltage which doesn't excess a (60 V). A digital thermometer or digital data logger type (CHINO with Digital Recorder 030) was used to record the temperature with range (0 – 1050 ^oC), and with an accuracy of (0.1 ^oC). It was coupled to a teletype–writer which prints a list of the temperatures and punches tape record of the data on the thermal papers.

4. RESULTS AND DISCUCCION

The results will be essentially divided into two categories; the flow results (friction factor), and the heat transfer results (Nusselt number, and axial temperature distributions). The apparatus was calibrated without using vortex generators to ensure its validity, and these

results were compared with the experimental results of the former investigations and gives a good agreement for the data of the (f) and Nu number. The parameters which are varied during the tests are: the number of generators, size of generators, location of generators, the angle of attack of the generators, and the Reynolds number.

4.1. Distributions of Axial Nusselt Number and Entrance Length Effect

Figure (4) is represented by local Nu number against the dimensionless axial coordinate (x / D_h) (x=0 represents the beginning point from the leading edge toward the other end of the test section), shows that the Nu number is relatively proportion with Re number and the thermal development is more rapid at lower Re number and slower at higher Re number. The lowermost curve (Re = 24,258) shows a shorter entrance length ($x/D_h \approx 9.8$) while it becomes greater as Re number increases until it is fixed after a value of (Re≈37,727).

This leads to say that the increase of the flow rate leads to an increase in the turbulence of flow, and the turbulence will destroy or penetrate deeper into boundary layer and especially in the corners regions (i.e., thinner the boundary layer the greater the heat transfer rate). Also, it is observed that the last two points of each run has an increase in the value of Nu number. This may be regarded to the excess heat losses within the last portion of the test section. This behavior is noticed also in ref [**9**].

The entrance length may be defined as the axial location at which the heat transfer coefficient approaches to within five percent of its fully developed value [**5**]. The values of the Nu number will have certain constant values at (Re≈37,000). This means that the entrance length will be nearly constant at this value of Re number as shown in Figure (5) which is represented by the dimensionless axial coordinate (x/D_h) while the abscissa is the Re number. These results give a good agreement with that of ref [**5**].

4.2. Fully Developed Nusselt Numbers

The values of Nu number in the investigation of Altemani–Sparrow, Petukhov–Popov, and Dittus–Boelter [**5**] which overpredicts the present data by about (7.8), (16.5–18.7), and (27.5–28.7) percent, respectively. The deviation (7.8 %) is accepted and expected because the cross–section of the present test section is similar to that used in the experiments of Altemani and Sparrow, whereas the other two deviations are large, and the reason is attributed to the difference of the cross–section of the heated duct. This comparison adds further confirmation that the results of Altemani and Sparrow have a superiority of comparison, and also it demonstrates that the hydraulic diameter does not provide an adequate rationalization of the noncircular geometry. This fact is also confirmed strongly by Chegini **[3]** results for asymmetrically heated tube. A simple formula of determined correlation is considered in ref [**5**] power–law fit correlation which is represented by Nu number as a function of Re number. The simplified form of the correlation of the Nu No is:

$$\overline{Nu} = f(\mathrm{Re}) \tag{1}$$

The above function is found to be in the following formula:

$$\overline{Nu} = b \,.\, (\mathrm{Re})^{c} \tag{2}$$

The index (c) equals to (0.781) as in ref. [**5**]. The fully development region is account only based on a five percent approach of heat transfer coefficient to its fully developed value. The correlation is to be:

$$\overline{Nu} = 0.0175 \,.\, (\mathrm{Re})^{0.781} \tag{3}$$

Whereas the correlation of Dittus-Boelter can be written as follow:

$$Nu = 0.023 \,.\, (\mathrm{Re})^{0.8} \,.\, (\mathrm{Pr})^{0.4} \tag{4}$$

This correlation was developed for circular tubes and is specified to be applicable for Re>10,000.

4.3. Transverse Heated Wall Temperature Distributions

Three thermocouples were installed in the cross–section of the heated wall at different four axial situations which are (1.4, 15.4, 26.6, and 40.6 D_h) from the leading edge of the test section. The measurements of transverse heated wall temperature are nearly symmetric. The maximum temperature is always observed near the corner regions (i.e., stagnation regions) due to low convection heat transfer, because of a thick boundary layer, whereas the minimum temperature occurs approach to mid length of heated wall–side due to high convection heat transfer rate because of a thin boundary layer.

The temperature at lower position of heated wall–side (i.e., at the corner between the heated and unheated wall) is slightly less than that at upper position of heated wall (i.e., the corner at an apex angle), because the temperature difference between the heated and unheated wall is large due to conduction heat transfer, whereas the heat balance occurs in the corner of an apex angle that means no conduction heat transfer.

Also, the first axial cross–section temperatures (i.e., at $x / D_h = 1.4$) are less than the others because the first cross–section lies in the entrance region that has a greater convection heat transfer coefficient and the other cross–sections lie in the fully development region that has a uniform convective heat transfer coefficient, see Figure (6).

4.4. Friction Factor Results

The main problem for the techniques of heat transfer enhancement inside channels lies in the large additional pressure drop associated with increase in heat transfer rate. The correlations of Blasius [**10**], Petukhov–Popov and Prandtl [**5**] are of circular tubes, whereas the correlations of Altemani–Sparrow [**5**] and Chegini–Chaturvedi [**3**] are of equilateral triangular ducts. The Blasius, Petukhov–Popov, Prandtl, and Chegini data over predict the present data by about (9.7, 8.8, 7.6, and 6.5) percent, respectively but the present data over predicts the data of Altemani–Sparrow by about (1.7) percent. The correlation of the friction factor is determined as a function of Re number and the simplified form of the present correlation is:

$$f = \phi(\mathrm{Re}) \tag{5}$$

The equation formula that is used in the former investigations can be written as following:

$$f = c\,/(\mathrm{Re})^{d} \tag{6}$$

The above equation can be written as following for the base case:

$$f = 0.2709 / \mathrm{Re}^{0.245} \quad (7)$$

Whereas the Blasius [**10**] and Chegini correlations for the smooth tube and equilateral triangular duct are written as following, respectively:

$$f = 0.316 / \mathrm{Re}^{0.25} \quad (8)$$

$$f = 0.305 / \mathrm{Re}^{0.25} \quad (9)$$

Depending on the above correlation for the(f), the constant parameter (c) will be used for comparison for different tests of friction factor values. The deviation between the equation (7) and the equations of (8) and (9) is of (9.96%) and (6.61%), respectively. The effect of the number of the vortex generators on the friction factor is shown in Figure (7).

It seems that the friction factor is reversely proportion with Re number and relatively proportion with number of the vortex generators, when the angle of attack of generators is fixed. The friction factor increases by about (8.87 %), (11.7 %), and (19.28 %) for (i, ii, iii) cases, respectively.

The change of the angle of attack of generators is one of the major influencing factors which affects on the (f). As the angle of attack of the vortex generator increases, the static pressure drop increases and thereby the (f) increases. The ratio of the (f) for (i, ii, iii) cases to that of the base case is plotted in Figure (8) when the abscissa is the angle of attack which are (6, 18, and 24 deg). For small values of angles of attack, the (f) increases slightly, but at great values of angle of attack (more than 18 deg), the (f) increases more rapidly because the area of the vortex generator across the flow direction increases (i.e., serves as an obstacle in the flow direction).

4.5. Heat Transfer Results

The parameter of the vortex generators which are varied is; the axial location before the leading edge of the heated duct, size, number, and the angle of attack of generators. Generally, exist of the vortex generators induces the creation of the streamwise longitudinal vortices behind it. The spiraling flow of these vortices serves to entrain fluid from their outside into their core. These vortices disrupt the growth of the thermal boundary layer and lead to enhance of heat transfer between the fluid and the heated walls of the duct.

The increase of the number of the vortex generators leads to increase the turbulence in fluid flow through a channel. Thus, many vortex generators are used to see the influence of the increasing of the turbulators area on the Nusselt number. The ratios of the augmentation in the Nu number can be obtained from case (i, ii, iii) by about (7.1 %), (10.45 %), and (13.47 %), respectively at (Re=56,896), when (β=18 deg).

The angle of attack of generators has an important role in the improvement of heat transfer. As investigated in ref [**7**], the Stanton number increases as the angle of attack increases until the angle reaches to (65 deg) for delta winglet pair type and then the St number decreases after this value. The case (III) has a good enhancement along the flow

direction at both low and high Re number. The results show that the Nu number increases by about (15.4 %), (24.1 %), and (28.5 %) for the angles (6, 18, and 24) deg respectively, at lower Re number. More figures for the other cases are published in the thesis ref [**11**].

The height of the vortex generators must be of the same order as the turbulent boundary layer thickness to disrupt the growth of the boundary layer and to generate a perturbed flows behind the vortex generators.

Therefore, two sizes are chosen during the experiments course; large and small size. The constant parameter (c) of the Nu correlation for the case (i, and I) as seen in the Figure (9) is fluctuated in explicit form. The reason is attributed to the tip of the vortex generators that is not sufficient to generate a turbulence flow and convert the corners regions from inert region to the active region in heat transfer.

The average fully developed Nu number of the three cases versus Re number are plotted in Figure (10) and compared with the base case at angle of attack of (18) deg. As shown, the Nu number increases with the airflow rate and the number of generators when the angle of attack is kept constant.

The location of the vortex generators plays an important role. Near the leading edge of the heated duct, there is a fact that the thermal boundary layer is so thin that it cannot be significantly perturbed by the vortex. Therefore, a (33.6 D_h) of the fully development section is used to allow the thermal boundary layer grows to the center of the duct before reaches to the leading edge of the heated duct. In other words, the hydraulic and thermal boundary layer is fully developed at the beginning point of the test section. From whole cases, after a certain length behind the vortex generator, the strength of the longitudinal vortices is reduced to a great extent although a spiraling flow still exists; due to the recirculation of the flow to repeat a mixing of the cooler stream of the core with the hot fluid from the wall. Therefore, another array of the vortex generators is almost needed after a distance of (25 D_h).

5. CONCLUSIONS

The friction factor data obtained here for base case has a low deviation compared with the Blasius [**10**], Petukhov-Popov and Prandtl [**5**] data for circular tubes, and as well as the data of Altemani-Sparrow [**5**] and Chegini-Chaturvedi [**3**] for noncircular ducts. The angle of attack of generators has a greater effect on a friction factor values than the number of the winglet-pairs as well as the size of generators.

Nusselt numbers were determined both in the thermal entrance region and in the fully developed region. The thermal entrance length increased with Reynolds number. Entrance lengths, based on a five percent approach to fully developed conditions, ranged from (14) to (17) hydraulic diameter over Reynolds number range from (24,000) to (58,000).

The experimentally determined fully developed Nusselt numbers for the base case were compared with the data of Altemani-Sparrow [**5**] for noncircular duct, and Petukhov-Popov and Dittus-Boelter data [**5**] for circular tubes (applicable for Re>10,000), with the hydraulic diameter replacing the tube diameter. The present data is less than that above by about (7.8), (16.5), and (27.5) percent respectively. Nusselt number ranges were improved greatly by changing the inclination angle values of generators and affected with less ratios of improvement by the number and the size of generators respectively.

ACKNOWLEDGEMENTS: The authors would like to acknowledge the Mechanical Engineering Department/University of Anbar, Mechanical Engineering Department/University of Tikrit, and Mechanical Department/Artistic Academy in Sakloeya who assisted our to facilitate and complete the laboratory rig.

REFERENCES

[1] Cengel, Y. A.," Heat Transfer A practical Approach", 1st Edition, Mic Groohil com., Inc., USA, 1998.

[2] Krieth Frank & Bohn Mark S., "Principles of Heat Transfer ", 5th Edition, PWS Publishing Company, a Division of International Thomson Publishing Inc.,1997.

[3] Chegini, H. & Chaturvedi, S.K., "an Experimental and Analytical Investigation of Friction Factors for Fully Developed Flow in Internally Finned Triangular Ducts", Journal of Heat Transfer, Vol. 108, August 1986, pp. (507– 512).

[4] Rohsenow, W.R., Hartnett, J.P., and Garric, E.N., "Handbook of Heat Transfer Applications", Vol.1, Chapter 7, McGraw–Hill, Inc., New York, 1985.

[5] Altemani, C.A.C., & Sparrow, E.M., "Turbulent Heat Transfer in an Unsymmetrically Heated Triangular Duct", ASME Journal of Heat Transfer, Vol. 102, November 1980, pp. (590 – 597).

[6] Pauley, W.R., & Eaton, J.K., "The Effect of Embedded Longitudinal Vortex Arrays on Turbulent Boundary layer Heat Transfer", Journal of Heat Transfer, Vol. 116, November 1994, pp. (871 – 879).

[7] Tiggelbeck, St., Mitra, N.K., & Feibig, M., "Comparison of Wing Type Vortex Generators for Heat Transfer Enhancement in Channel Flows", ASME Journal of Heat Transfer, Vol. 116, November 1994, pp. (880 – 885).

[8] ASHRAE "ASHRAE Handbook", Chapter Three, Millstar Electronic Publishing Group, Inc., 1997.

[9] Hassan, A. K. A., "Forced Convection in Isosceles Right Angle Triangular and 4–Cusp Ducts", Ph.D. Thesis, Department of Mechanical Engineering, University of Liverpool, 1984.

[10] Streeter Victor L. & Wylie E. Benjamin, "Fluid Mechanics ", 7th Edition, McGRAW–HIL, Inc., 1979.

[11] Zangana, H. E., "Effect of Delta–Winglet Vortex Generators on a Forced Convection Heat Transfer in an Asymmetrically Heated Triangular Duct", Msc. Thesis, Mechanical Engineering Department, University of Anbar, 2005.

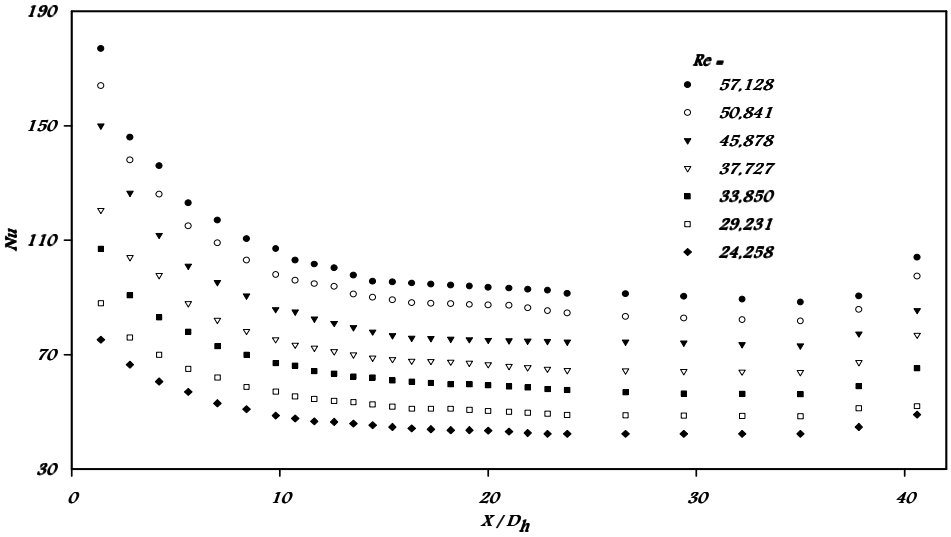

Fig. 4. Axial distribution of the Nu number for base case.

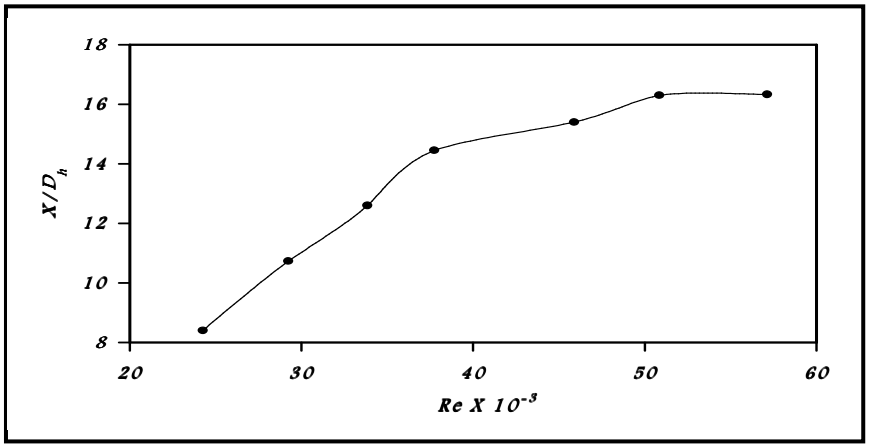

Fig. 5. Thermal entrance lengths for the base case.

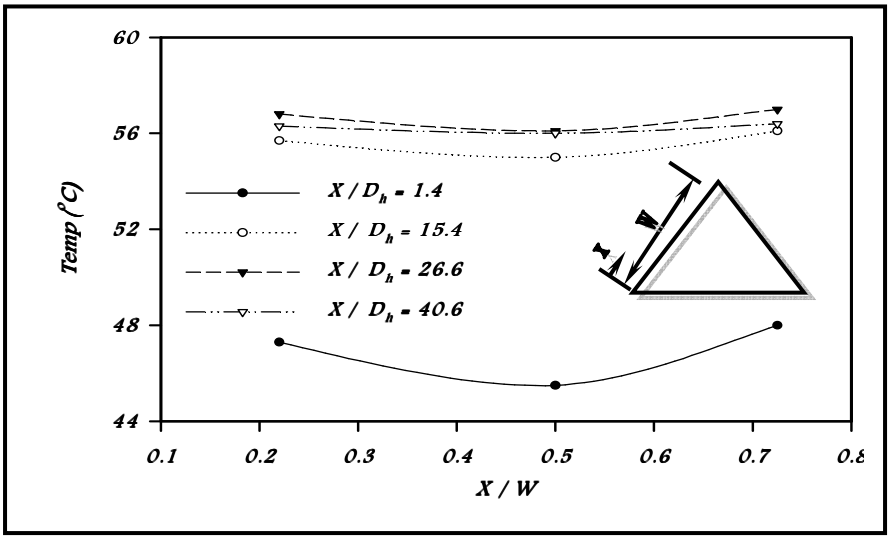

Fig. 6. Transverse heated wall temperature distribution at four axial situations, (Re=29,950).

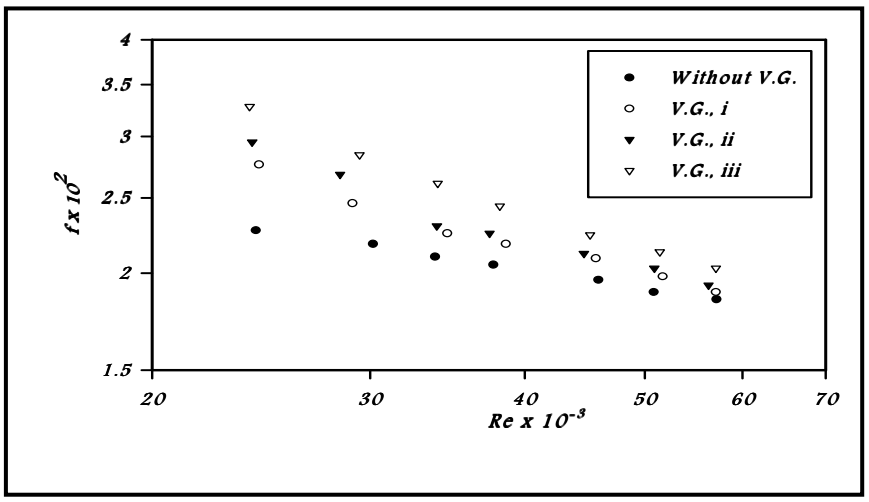

Fig. 7. Effect of generators number on a friction factor at θ=18 deg.

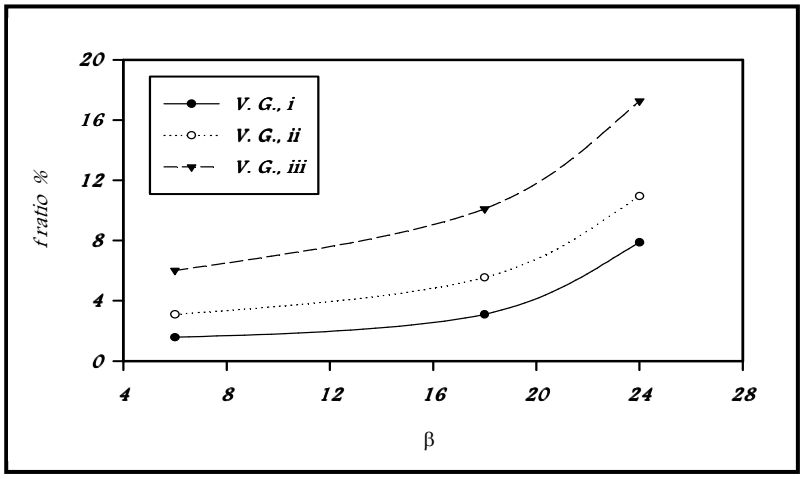

Fig. 8. Ratio of (f) to the (f) for base case at Re=54,000.

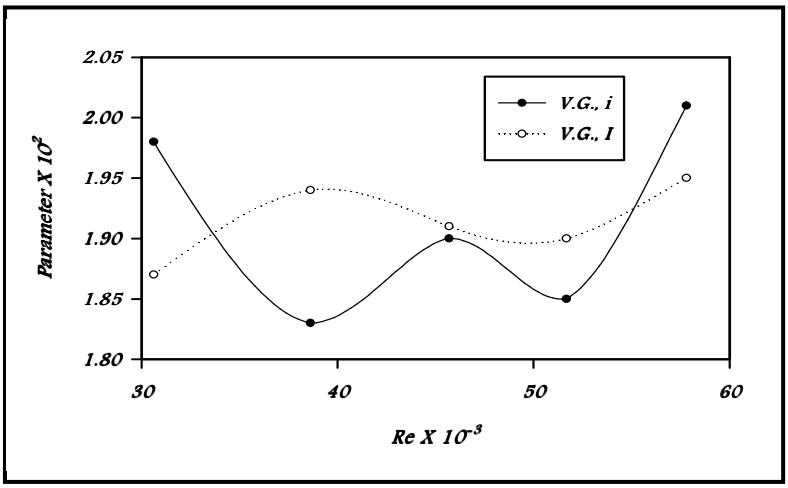

Fig. 9. The parameter of the Nu number correlation versus Re number.

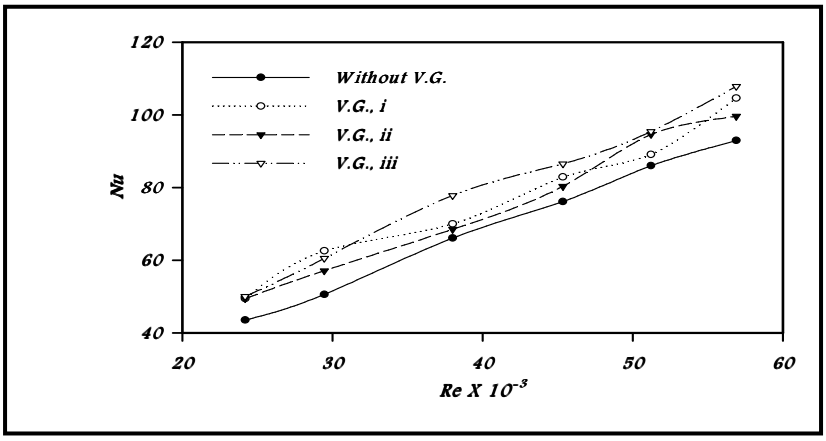

Fig. 10. Axial distributions of the Nu number.